Tellus (2006), 58A, 473–486
Printed in Singapore. All rights reserved

TELLUS

The use of a calculus-based cyclone identification method for generating storm statistics

By R. E. BENESTAD[1]* and D. CHEN[2,3], [1]*The Norwegian Meteorological Institute, PO Box 43, 0313, Oslo, Norway;* [2]*Earth Sciences Centre, Gothenburg University, Sweden;* [3]*Laboratory for Climate Studies/National Climate Center, China Meteorological Administration, Beijing, China*

(Manuscript received 8 December 2005; in final form 24 March 2006)

ABSTRACT

Maps of 12 hr sea-level pressure (SLP) from the former National Meteotrological Center (NMC) and 24 hr SLP maps from the European Centre for Medium-range Weather Forecasts (ECMWF) 40 yr re-analysis (ERA40) were used to identify extratropical cyclones in the North Atlantic region. A calculus-based cyclone identification (CCI) method is introduced and evaluated, where a multiple regression against a truncated series of sinusoids was used to obtain a Fourier approximation of the north–south and east–west SLP profiles, providing a basis for analytical expressions of the derivatives. Local SLP minima were found from the zero-crossing points of the first-order derivatives for the SLP gradients where the second-order derivatives were greater than zero.

Evaluation of cyclone counts indicates a good correspondence with storm track maps and independent monthly large-scale SLP anomalies. The results derived from ERA40 also revealed that the central storm pressure sometimes could be extremely deep in the re-analysis product, and it is not clear whether such outliers are truly representative of the actual events. The position and the depth of the cyclones were subjects for a study of long-term trends in cyclone number for various regions around the North Atlantic. Noting that the re-analyses may contain time-dependent biases due to changes in the observing practises, a tentative positive linear trend, statistically significant at the 10% level, was found in the number of intense storms over the Nordic countries over the period 1955–1994 in both the NMC and the ERA40 data. However, there was no significant trend in the western parts of the North Atlantic where trend analysis derived from NMC and ERA40 yielded different results. The choice of data set had a stronger influence on the results than choices such as the number of harmonics to include or spatial resolution of interpolation.

1. Introduction

Cyclones are important synoptic systems that have a significant impact on weather and society. On the synoptic scales, cyclones and anticyclones account for most of the atmospheric variability in mid- latitudes (Trenberth, 1991). The study of cyclones is not only of practical importance since they are a source of severe weather including heavy rain and strong winds, but also of theoretical importance since they are an important agent for transport of energy, momentum and water vapour in the climate system, thereby playing an important part in the mean-wave flow interaction (Peixoto and Oort, 1992). One aspect that complicates the understanding of the cyclones, is the difference between tropical and mid-latitude systems. In the Tropics, convective instabilities are more important whereas in mid-latitudes the cyclones are driven rather by baroclinic instabilities. In both cases, conversion from latent heat is a primary energy feeding mechanism. The focus of this paper will be on the mid-latitude cyclones.

Manual identification and investigations of cyclones in mid-latitudes started when synoptic weather maps were systematically prepared in the 1850s. Studies on cyclones began fairly early (e.g. Mohn, 1870). However, it took some time for a comprehensive and systematic analysis to be realized, which took place in the mid-twentieth century (e.g. Petterssen, 1950). With the development and extensive application of the digital sea-level pressure (SLP) data, automatic tracking algorithms became a necessity (e.g. Leonard et al., 1999). These algorithms have recently been developed to facilitate an objective and consistent description of cyclone climatology (Murray and Simmonds, 1991; Jones and Simmonds, 1993; Blender et al., 1997; Grigoriev et al., 2000).

The identification of cyclones depends on the algorithms and input data used, and different algorithms may give different results. In addition, data quality, time and space resolution of

*Corresponding author
e-mail: rasmus.benestad@met.no
DOI: 10.1111/j.1600-0870.2006.00191.x

the input data have an impact on the results of cyclone tracking (Blender and Schubert, 2000). Although re-analysis can be regarded as the best representation of the global atmosphere, use of different re-analysis products can still lead to different results. For example, Hanson et al. (2004) show that although the statistics of the cyclone tracks based on European Centre for Medium-range Weather Forecasts (ECMWF) and National Center for Environmental Prediction (NCEP) re-analysis are similar, there can be some differences in temporal evolution of the identified individual cyclones.

Many recent works show that cyclone properties vary on a variety of timescales (Alpert et al., 1990; Agee, 1991; Gulev et al., 2001; Sepp et al., 2004; Zhang et al., 2004). The detection of trends in cyclone statistics is complicated by pronounced interannual and decadal variations (Walsh, 2004). While some studies have not found significant trends in the mid-latitude storminess (Hall et al., 1994; Carnell and Senior, 1998; Schubert, 1998; Key and Chan, 1999; Ulbrich and Christoph, 1999; Graham and Diaz, 2001), others suggest that there may have been long-term trends in some regions (Geng and Sugi, 2001; Gulev et al., 2001; Fyfe, 2003; Zhang et al., 2004). It is worth keeping in mind that different extratropical regions may experience different trends in the storm numbers and intensities if the storm track is displaced. Geng and Sugi (2001) noted that an increase in the cyclone density over the North Atlantic (45°–80° N, 60° W–0° E) and the cyclogenesis may be associated with the large-scale baroclinicity. Since the meridional temperature profile sets the thermal wind, the large-scale baroclinicity is influenced by the large-scale temperature structures. Geng and Sugi (2001, 2003) inferred from model-based studies of mid-latitudinal storms, a relationship between the level of mid-latitude cyclone activity and the condition for baroclinic instabilities, and Geng and Sugi (2003) suggested that an enhanced greenhouse effect may lead to a reduction of the number of weak and medium-strength extratropical cyclones and an increase in strong cyclones. Fyfe (2003) noted a small increase in the number of deep cyclones, as well as a decrease in the number of cyclones over the sub-Antarctic Ocean (40°–60° S) and a weak increase over the Antartic Ocean (60°–90° S) during the period 1960–1999. Gulev et al. (2001) found an increase in the number of cyclones in the Arctic and over the western Pacific as well as a decrease over the Gulf Stream and subpolar Pacific. Zhang et al. (2004) found an increase of the number and intensity of cyclones moving into the Arctic from the mid-latitudes, and suggested that there has been a shift in the storm tracks into the Arctic. Alexander et al. (2004) used a climate model (CCM3.6) to study cyclones, and found that the North Atlantic storm track activity is enhanced by an ice-cover retreat in the Greenland-Iceland-Norwegian (GIN) Seas. Thus, a trend in the mid-latitude storm statistics may be consistent with changes in the sea-ice extent (Meier et al., 2005). One caveat is that climate models (AOGCMs) tend to have low spatial resolution which may affect their ability to adequately represent the cyclone frequencies as well as individual storm characteristics (Jung et al., 2006).

According to Walsh (2004), there is a large number of cyclone detection schemes relying on combinations of threshold values used for detecting cyclone-like vortices in general circulation models (GCMs), but there appears to be no genuinely objective means for setting these threshold values. Alternatively, storm activity is expressed in terms of short-term variance for a given location over time, the so-called Eulerian approach (Hoskins and Hodges, 2005). For instance, Geng and Sugi (2003) used smoothed 2–7 d 500 mb vertical velocity variance as an indicator of the storm activity, and Sorteberg et al. (2005) identified storm tracks by searching for positive 850 hPa vorticity anomalies, in order to study track densities and mean intensity.

It is important to keep in mind the distinction between estimating the trajectories of the systems (storm tracks diagnostics) and identifying the storm centres (also referred to as 'feature points'). Whereas a sophisticated 'feature tracking' scheme may be used for analysing storm tracks (e.g. Hodges, 1999; Hoskins and Hodges, 2002, 2005), the identification of actual storm centres may be more primitive. Zhang et al. (2004) used a conventional-type cyclone identification method consisting in identifying cyclones by comparing grid point values with its eight surrounding values, but they set an additional criterion that the minimum difference between the centre value and the surrounding points after smoothing ('SLP gradient') must be greater than a threshold value (0.15 hPa). Hoskins and Hodges (2002) compared 2–6 d bandpass type approaches to a feature tracking approach (Hodges, 1995), and concluded that tracking diagnostics give some details not readily available from Eulerian studies.

The calculus-based cyclone identification (CCI) method used in this study is more complicated than many of the earlier methods (Gulev et al., 2001; Zolina and Gulev, 2002; Geng and Sugi, 2003), but is also more computationally demanding (it can nevertheless be done on a modern PC or workstation). In some respect, the CCI method is comparable with more elaborate cyclone analyses, such as involving B-splines (Hodges, 1994, 1995) or the Laplacian of pressure surface (Simmonds and Murray, 1999; Simmonds and Keay, 2000). The B-splines ('B' for 'basis') involves a recursive fitting of piecewise polynomials rather than a least-squares multiple regression fit to an analytical solution provided by a truncated Fourier series. The CCI approach used here works in a similar fashion as the B-splines (Hodges, 1995) in terms of fitting smooth functions and interpolation, but offers the advantage of providing explicit analytical solutions for the gradients estimated through a regression analysis. Here, harmonics are used instead of polynomials for providing a smooth interpolation. The method employed by Hodges (1994, 1995) provided either an interpolating surface or a least-squares approximation, depending on the parameters used. The CCI method provides

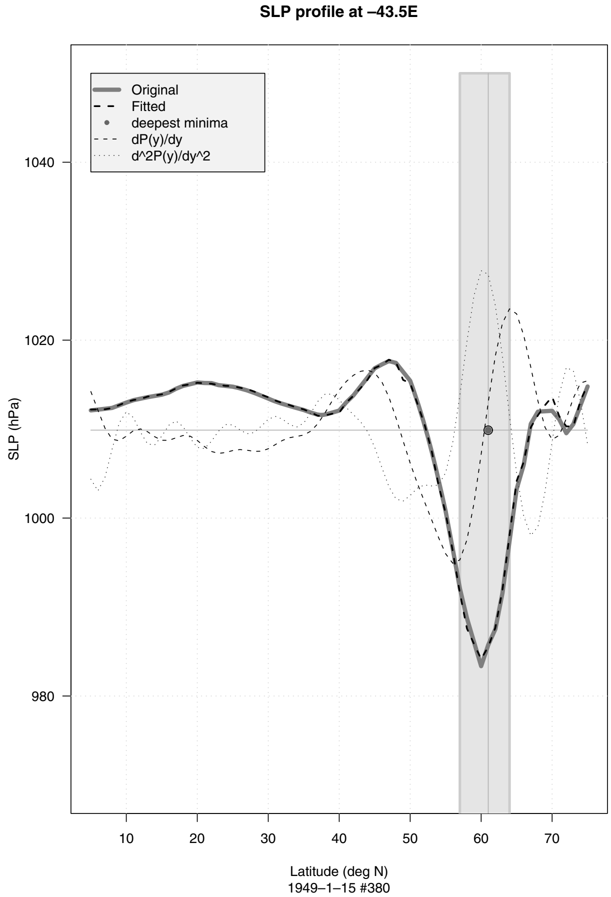

Fig. 1. Test of the identification procedure for local minima in the pressure profiles along any meridional line. The data are represented by the thick grey line and the dashed line shows the Fourier approximation. The solid circle on the dashed line marks the position of the deepest local minimum. The identification algorithm was based on zero first derivatives, positive second derivatives and equation 2. The first and second derivatives have been rescaled for the case of clarity on this plot. These results were derived from ERA40 SLP.

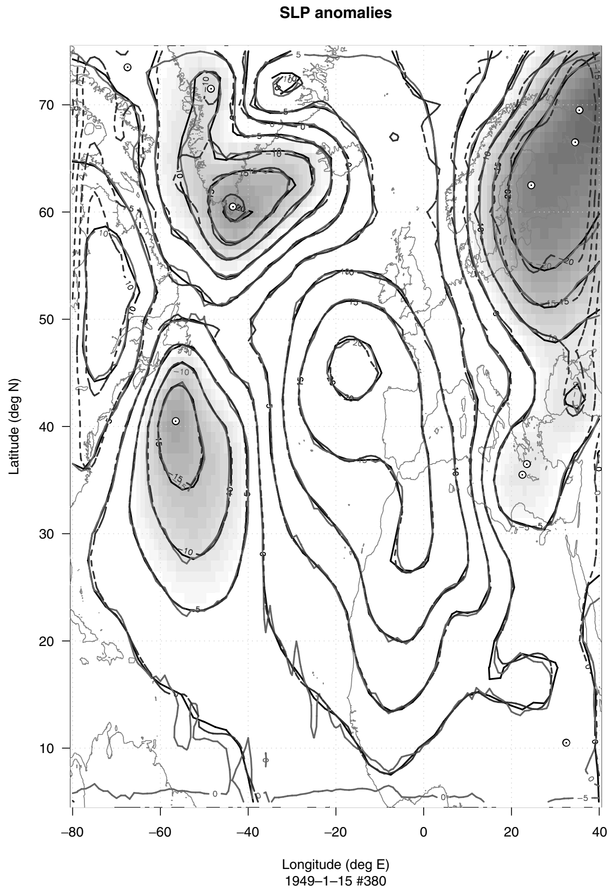

Fig. 2. Test of the identification procedure for local-lows showing the location of local minima in the 2-D SLP field. These results were derived from ERA40 SLP.

both a least-squares approximation of the SLP surface employing ordinary least-squares regression (other types of regression can in principle be used), and these approximate surfaces are then utilized for spatial interpolation (this can be seen in Figs 1 and 2). Hodges (1994) used an *ad hoc* method for identifying centroids of feature points, and Hodges (1995) later improved the feature-point identification by applying a combination of interpolation/smoothing and local maximization to compute off-grid local maxima or minima. Hodges (1994, 1995) focused mainly on tracking whereas the analysis presented here focus on the feature identification and the evaluation of the cyclone feature statistics. The CCI also differs from the B-splines approach by defining the local minima as the zero-crossing points of the derivatives. The CCI approach also bears some similarities to the work of Simmonds and Keay (2000) and Simmonds and Murray (1999), who used local maxima of the Laplacian of pressure to identify cyclones. Their method involved a spatial smoothing and employed an iterative approximation to fit the centre of the ellipsoid that best fit the pressure surface defined by a bi-cubic spline function. The CCI method is arguably more mathematically rigorous as it seeks solutions consistent with the form e^{ikx} that is common to many differential equations, and it provides an analytical solution to the pressure gradients based on a truncated Fourier series, for which the values for the coefficients are estimated using a linear multiple regression. Furthermore, the Simmonds and Keay (2000) and Simmonds and Murray (1999) analyses were applied to the southern hemisphere whereas present analysis focus on the Nordic region. In theory, spherical harmonics—Legendre functions—could be employed, however, it would involve complicated and computationally demanding calculations (Hodges, 1995). A simple cylindrical projection is used here, as it is considered adequate for mid-latitude storms as long as the Polar region is excluded (Hodges, 1994). For a more general analysis, a spherical coordinate system for the data (Hodges, 1995) is superior, however, a polar stereographic projection (Simmonds and Murray, 1999; Simmonds and Keay, 2000) can also be used for the high latitudes.

Hoskins and Hodges (2002, 2005) used least squares fit to spherical harmonical functions to remove the background field, but not for detecting local minima (maxima). Since we were interested in SLP gradients (gradient winds) and we could not think of a good reason why we should remove the background field before applying our method, the CCI analysis was applied to the total SLP here.

The main purpose of this paper is to introduce a new cyclone identification method, but we also wanted to provide regional storm statistics and search for trends over the Nordic countries—hence the focus on this region. The outline of this paper is as follows: A description of the data used followed by a detailed

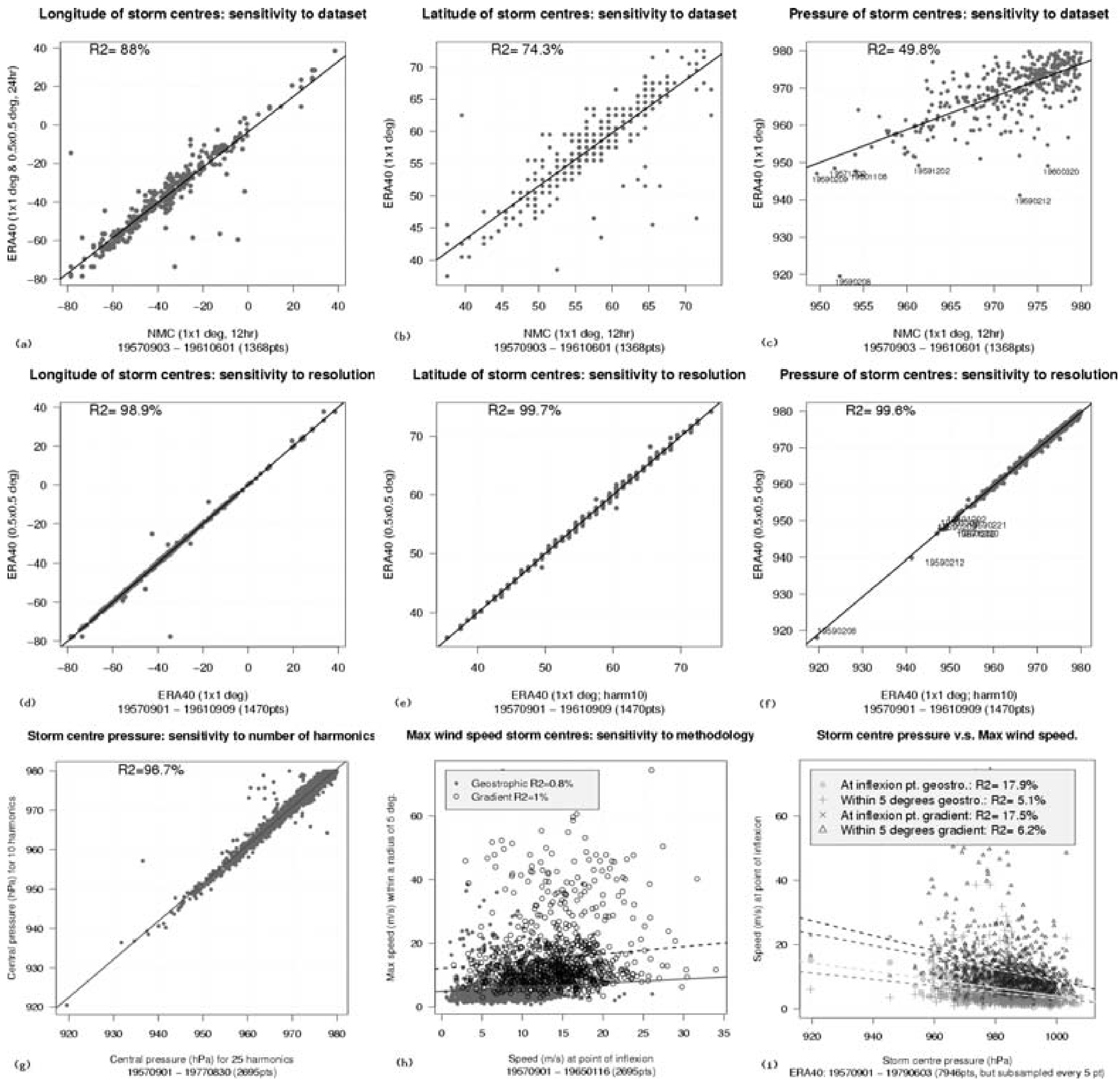

Fig. 3. Sensitivity of the derived storm characteristics to choice of dataset (a–c), resolution used for interpolation (d–f), number of harmonics (g), and method for estimating maximum speed (h–i). The date (YYYMMDD) is given in panels c and f for the cyclones with a central pressure below 950 hPa. The four different methods for estimating maximum geostrophic wind speeds was taking the maximum values estimated (i) within a radius of 5 degrees, (ii) at the points of inflexion (see Fig. 1), and the gradient winds estimated (iii) within a radius of 5 degrees and (iv) at the points of inflexion. The SLP were taken at 12:00 UTC for both NMC and ERA40.

presentation of the CCI method. The ‘Data and Method’ section is followed by a ‘Results’ section presenting the evaluation of the CCI-method, and ‘Discussion’ concludes our analysis.

2. Data and Method

2.1. Data

The data used to derive the cyclone statistics was taken from the (24 hr) ECMWF 40 yr (1958–2002) re-analysis (ERA40) (Simmons and Gibson, 2000; Simmons et al., 2004; Uppala et al., 2005) SLP (taken at 12:00 UTC) and the gridded ds195.5 SLP data set of 12 hr (taken at 00:00 and 12:00 UTC) SLP (1955–1994) from the National Meteorological Center (NMC), now National Center for Environmental Prediction (NCEP). It is not certain that the SLP is the most appropriate parameter for identifying cyclones in general (Hoskins and Hodges, 2002), however, it is nevertheless arguably one of the parameters with the most complete observational records as well as among the most constrained parameters in the re-analysis products (in regions with high quality observations) since observed surface pressure is used in the assimilation whereas vorticity is a model-derived quantity. Furthermore, the SLP is measured directly and provides a convenient basis for validation in terms of the location of low-pressure systems. Another advantage with SLP is that gridded synoptic data reconstruction can extend further back in time than derived fields like vorticity, since SLP fields can be derived from empirical (historical) surface pressure alone. One important difference between the NMC and ERA40 data is that the former is derived through a number of different statistical analyses as well as using a forecast model (T126L18) whereas the latter is produced by one single state-of-the-art atmospheric GCM (T159L60 including the stratosphere) that has assimilated a wider range of past observations (the number of observations has changed over time). The spatial resolution of both the NMC and the ERA40 data used here is $2.5^\circ \times 2.5^\circ$ (the original ERA40 data is produced with a higher spatial resolution). A conversion to the Unidata’s netCDF format (Rew et al., 1996) and subsequent evaluation of the NMC data set was carried out documented by Benestad (1998). For empirical downscaling, the `R`-package `clim.pact` (Benestad, 2004) was used, together with SLP re-analysis from the NCEP (Kalnay et al., 1996).

2.2. Method for cyclone identification

Instead of comparing each grid-point value directly with its nearest neighbours to identify low-pressure systems, the CCI method involves multiple least-squares regression to a truncated series of sinusoids in order to estimate the values of the coefficients in a Fourier approximation. It is also possible to compute gradients from Fast Fourier Transformed (FFT) profiles, although not done here. Local minima are found along north–south and east–west profiles of SLP by solving for the first and second order

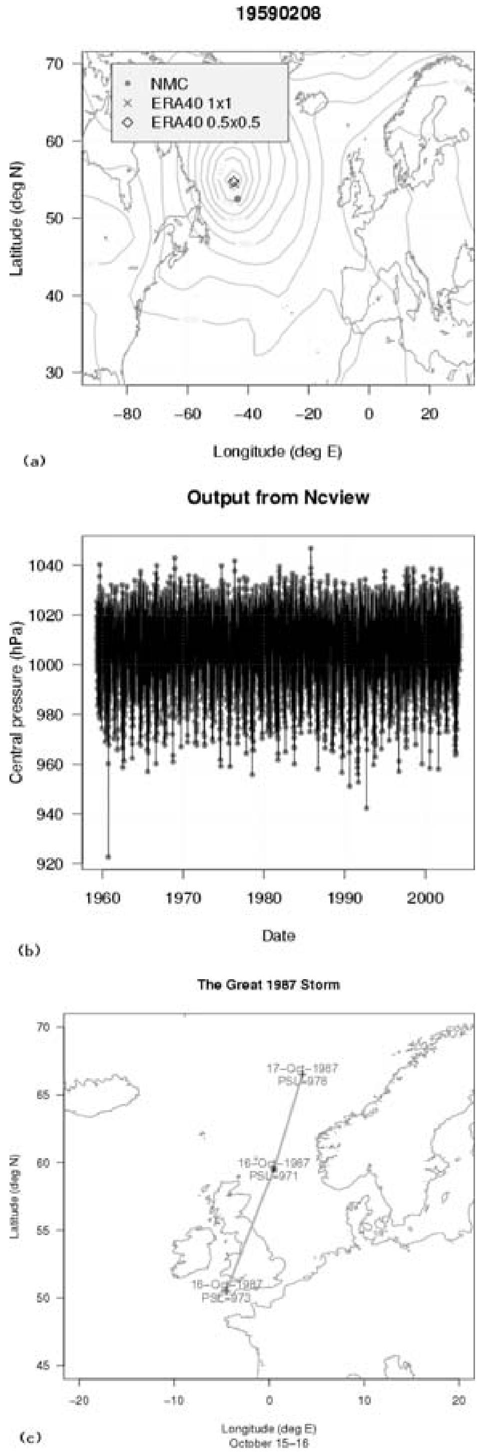

Fig. 4. Case study: (a) Location of 8 February 1959 (b) SLP time-series (time-series plotted and dumped to a separate file with an independent tool Ncview 1.92 d by David W. Pierce, and then replotted the same results in R for improving the picture quality), and (c) the track for the Great Storm of 1987. In panel (a), four points are plotted: NMC, ERA40 at 1×1 degree resolution and ERA40 at 0.5×0.5 degree resolution.

derivatives and searching for zero crossing for the former and positive values for the latter. The calculation of derivatives is a modification of the method used by Benestad and Hanssen-Bauer (2003) to compute the slope associated with the Fennoscandian topography and the technique for differentiation of power series (polynomials) used in Benestad (2003). A mathematical description and an evaluation of the cyclone identification method is given below.

Let the SLP P be a 2-D field: $P(x, y)$ or $P(\theta, \phi)$ in terms of spherical polar coordinates where θ is the longitude and ϕ the latitude. Local pressure minima can then be found using $\partial P/\partial x = \partial P/\partial y = 0$ and $\partial^2 P/\partial x^2 > 0$ and $\partial^2 P/\partial y^2 > 0$. Let $p(\theta)$ represent a profile of $P(\theta, \phi)$ along the zonal direction and $p(\phi)$ be a profile along the meridional. A Fourier approximation can be obtained for $p(\theta)$ and $p(\phi)$:

$$p(\theta) = p_0 + \sum_{i=1}^{N_\theta}[a_\theta(i)\cos(\omega_\theta(i)\theta) + b_\theta(i)\sin(\omega_\theta(i)\theta)],$$
$$p(\phi) = p_0 + \sum_{i=1}^{N_\phi}[a_\phi(i)\cos(\omega_\phi(i)\phi) + b_\phi(i)\sin(\omega_\phi(i)\phi)], \quad (1)$$

where the number of harmonics fitted were $N_\theta = N_\phi = 25$. The index variables are given as $\theta = \theta_1, \theta_2, \ldots \theta_n$ (step size $\delta\theta = \theta_2 - \theta_1$ over interval: $\Delta\theta = \theta_n - \theta_1$) along the longitudes and $\phi = \phi_1, \phi_2, \ldots \phi_m$ (step size $\delta\phi = \phi_2 - \phi_1$ over interval: $\Delta\phi = \phi_m - \phi_1$) for the latitudes. The spatial scales are controlled by θ and $\omega_\theta(i) = 2\pi i/(\Delta\theta)$ along the longitude and ϕ and $\omega_\phi(i) = 2\pi i/(\Delta\phi)$ along the latitude. The coefficients $a_\theta(i)$, $b_\theta(i)$, $a_\phi(i)$, and $b_\phi(i)$ are estimated here through a multiple linear regression scheme, although an FFT can also be employed. The constant terms p_0 represent an arbitrary constant that may vary from profile to profile, and the regression-based estimates of the coefficients will henceforth be denoted as $\hat{a}_\theta(i)$, $\hat{b}_\theta(i)$, $\hat{a}_\phi(i)$, and $\hat{b}_\phi(i)$ respectively. Using the best-fit Fourier approximation, the derivatives can easily be solved by following analytical expressions:

$$\frac{d\hat{p}(\theta)}{d\theta} = \sum_{i=1}^{N_\theta}\omega_\theta(i)[-\hat{a}_\theta(i)\sin(\omega_\theta(i)\theta) + \hat{b}_\theta(i)\cos(\omega_\theta(i)\theta)],$$

$$\frac{d\hat{p}(\phi)}{d\phi} = \sum_{i=1}^{N_\phi}\omega_\phi(i)[-\hat{a}_\phi(i)\sin(\omega_\phi(i)\phi) + \hat{b}_\phi(i)\cos(\omega_\phi(i)\phi)]. \quad (2)$$

The second derivative was estimated by repeating the differentiation described in equations 2. Since the coordinates were expressed in spherical polar coordinates (Gill, 1982, p. 94), the zonal (x) and meridional (y) gradients were solved according to

$$\frac{d\hat{p}(x)}{dx} = \frac{1}{a\cos(\phi)}\frac{d\hat{p}(\theta)}{d\theta},$$
$$\frac{d\hat{p}(y)}{dy} = \frac{1}{a}\frac{d\hat{p}(\phi)}{d\phi}, \quad (3)$$

where $a(=6.378 \times 10^6 m)$ is the mean radius of the Earth. The ERA40 data is available at the model resolution of $1^\circ \times 1^\circ$, but a truncated version was used here because a lower resolution requires less memory and speeds up the computations (by reducing the number of input-output operations). Prior to the fitting of harmonics, however, the gridded SLP data of both NMC and ERA40 had been interpolated onto a finer ($1^\circ \times 1^\circ$ or higher resolution in some of the evaluation exercises) grid employing a bilinear interpolation scheme (The function `interp` in the R-package `akima`) implying smaller values for $\delta\theta$ and $\delta\phi$, thus providing a higher fidelity for the cyclones location. It is in principle also possible to use the original resolution of the SLP to obtain the Fourier coefficients in equation 1, and then change $\delta\theta$ and $\delta\phi$ to obtain a higher resolution. The truncation of the spatial resolution of the ERA40 re-analysis may affect the number of shallow cyclones (Jung et al., 2006), but the subsequent expansion in terms of spatial resolution (for both NMC and ERA40) may partially compensate for this. The resulting higher

Table 1. Cross-correlation of annual cyclone count in the seven different regions: $N = 40$, and the 95% confidence interval for an iid series is estimated to be ±0.3 sampling 1000 series of stochastic numbers (random number generator). The keys 'Nordic', 'Deep', and 'Weak' denote the Nordic region (5° E–35° E/55° N–72° N), but with different threshold values (1000, 980 and 1020 hPa respectively), whereas 'Iceland' refers to 40° W–0° E, 55° N–67° N, 'Europe' to 10° W–20° E, 40° N–55° N, 'Newfoundland' to 70° W–30° W,50° N–65° N, 'Bermuda' to 80° W–40° W, 35° N–50° N, and 'Subtropical Storms' to 80° W–30° W, 35° N–50° N, with a threshold value of 970 hPa. The analysis is based on the *annual* NMC counts and is, therefore, not affected by common seasonal variations.

	Nordic	Deep	Weak	Iceland	Europe	Newfoundland	Bermuda	Subtropical Storms
Nordic	**1.00**	**0.61**	**0.84**	**0.36**	−0.11	**0.36**	0.01	−0.18
Deep	**0.61**	**1.00**	**0.33**	**0.38**	**−0.30**	0.25	−0.24	**−0.39**
Weak	**0.84**	**0.33**	**1.00**	**0.35**	0.13	**0.42**	**0.33**	0.05
Iceland	**0.36**	**0.38**	**0.35**	**1.00**	0.03	**0.83**	−0.02	−0.07
Europe	−0.11	**−0.30**	0.13	0.03	1.00	0.09	**0.47**	**0.57**
Newfoundland	**0.36**	0.25	**0.42**	**0.83**	0.09	**1.00**	0.22	0.04
Bermuda	0.01	−0.24	**0.33**	−0.02	**0.47**	0.22	1.00	**0.30**
Subtropical Storms	−0.18	**−0.39**	0.05	−0.07	**0.57**	0.04	**0.30**	1.00

resolution nevertheless provides higher precision in the location of the storm centres.

When the maps are constructed from gridded data, there is a risk of undercount due to storms skipping grid boxes when the temporal resolution is low (Zolina and Gulev, 2002). In the present analysis, the maps were sampled into 30×30 bins, corresponding to 8 degrees or $\sim$230 km at 75° N (the critical speed above which this skipping effect becomes significant is 2.7 m s^{-1} for 24 hr values and 5.4 m s^{-1} for 12 hr values at 75° N, but it increases at lower latitudes). Skipping may be a problem for tracking cyclones, but since we focused on other properties such as variations in the cyclone number/day and SLP gradients, skipping will have a similar effect as subsampling.

The Fourier approximation is applied to north-south and east-west lines respectively, and the cyclones are identified where local minima in the north-south line coincide with the local

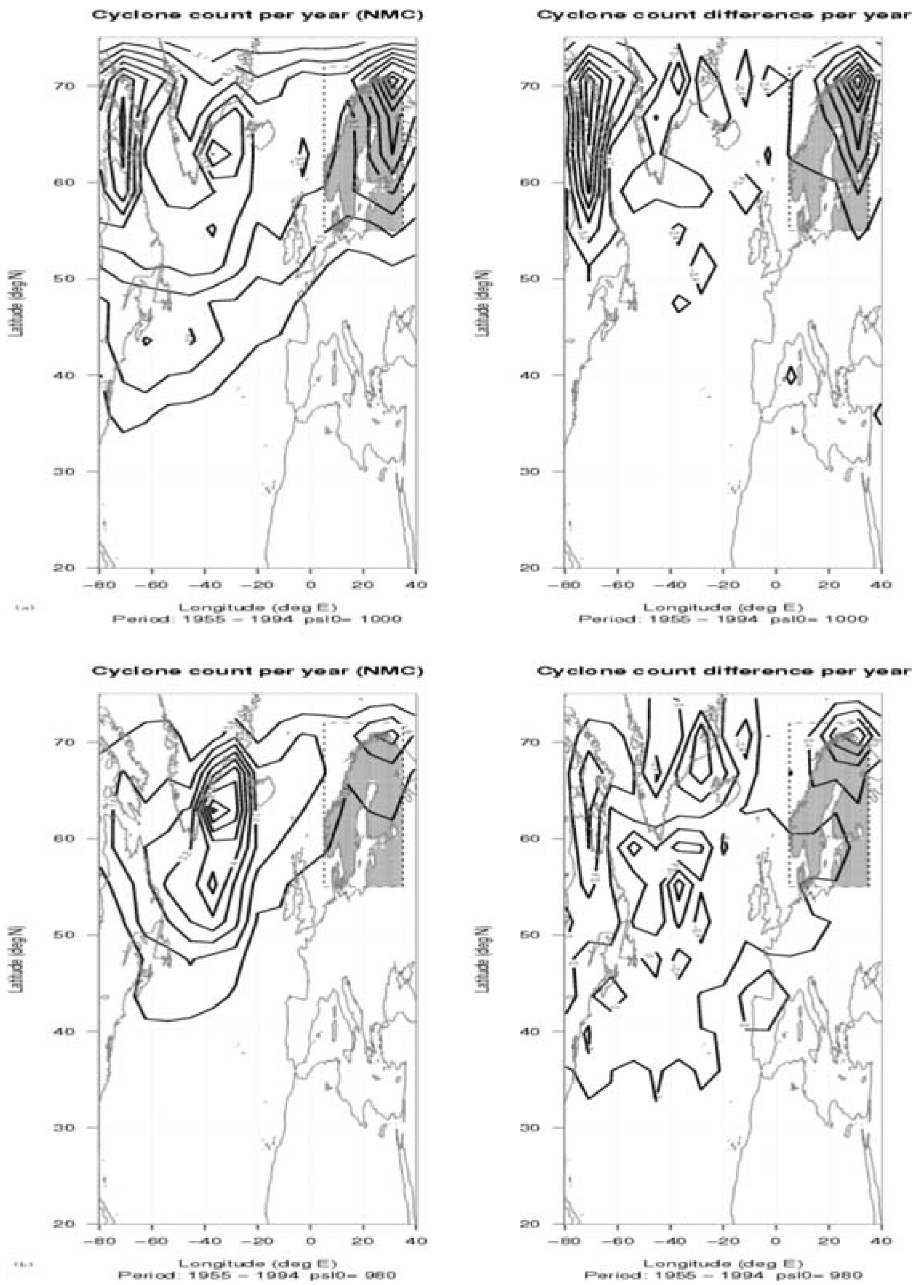

Fig. 5. Map of cyclone density over the North Atlantic, showing the familiar storm track for cyclones with local SLP minima < 1000 hPa (upper) and cyclones with local SLP minima < 980 hPa (lower). Left panels show the count derived from NMC and the right panels show the difference between the storm count from NMC and ERA40 (NMC-ERA40).

Table 2. Trend summary for different regions and different threshold SLP, for both the NMC data and the ERA40. '+/+' means a positive trend in both results (5% signf.), '0/−' means zero trend in the NMC and a negative trend in the ERA40 results. '+' or '−' in parenthesis indicate weak trends (10% signf.). 'Nordic' =5° E–35° E/55° N–72° N, 'Bermuda' = 80° W–30° W/35° N–50° N, 'Europe' = 10° W–20° E/40° N–55° N, 'Newfoundland' = 70° W–30° W/50° N–60° N, 'Iceland' = 40° W–0° E/55° N–67° N, 'Subtropical Storms' = 80° W–30° W, 35° N–50° N, and 'N. Atl.' = 80° W–40° E/20° N–50° N. The linear trend is done for monthly cyclone counts—regression.

Region	SLP							
	950 hPa	960 hPa	970 hPa	980 hPa	990 hPa	1000 hPa	1020 hPa	1030 hPa
Nordic		(+)/0	(+)/0	(+)/(+)	(+)/(+)	(+)/0	(+)/0	(+)/0
Europe				0/0	0/0	0/(−)	0/(−)	
Iceland				(+)/(+)	(+)/0	0/(+)	0/(+)	
Bermuda				0/(−)	0/(−)	0/0	0/(−)	
Newfoundland				(+)/0	(+)/0	0/0	(+)/0	
Subtropical Storms	0/0	0/0	0/(−)	0/0				
N. Atl.				(+)/0	(+)/0	0/(−)	0/0	

minima in the east-west line. The local minima in either line were taken at the zero crossing of the first derivatives (thin dashed line in Fig. 1), and the precision of the cyclone location can be increased by choosing small values for $\delta\theta$ and $\delta\phi$.

Figure 1 provides a test of how well the Fourier truncation (thick black dashed) relates to the data (thick grey; ERA40) and demonstrates how well a minimum is located at the zero crossing for the first derivative (marked with a filled circle). The dotted line in Fig. 1 marks the points of inflexion (points where $\partial^2\hat{p}/\partial x^2 = 0$ or $\partial^2\hat{p}/\partial y^2 = 0$) and the grey region marks the range between the two closest points of inflexion on either side of the storm centre. The radius (r) of the storm was taken as the minimum distance between storm centre location and points of inflexion, estimated along the north–south and the east–west profiles respectively. The SLP gradients were used to compute the geostrophic wind speed associated with the storms, taking the wind speed to be $v_g(\phi) = [\sqrt{(\partial p/\partial y)^2 + (\partial p/\partial x)^2}]/[f(\phi)\rho]$, assuming $\rho = 1.293$, and $f(\phi) = 0.000147 \sin(\pi\phi/180)$. Four different methods were tried for estimating the maximum wind speed near the storm: (i) taking the maximum value for $v_g(\phi)$ within 5 degree radius, (ii) taking the maximum of the geostrophic wind speed estimated at the four points of inflexion, (iii) computing the gradient wind (Fleagle and Businger, 1980, p. 161) within 5 degree radius and (iv) at the inflexion points. The gradient wind was estimated according to the expression $V(\phi) = -0.5 f(\phi) r[1 \pm \sqrt{1 + 4v_g(\phi)/(f(\phi)r)}]$.

In this study, the CCI-method was restricted to counting 10 simultaneous cyclones in the region 80° W–40° E, 20°–75° N, although many more simultaneous storms systems may in principle be accounted for. Figure 2 shows the location of local minima in relation to a contour plot of SLP for a random day. The statistics presented in the subsequent discussion excludes weak cyclones (local minimum pressure greater than 1000 hPa) unless otherwise stated. No filtering was applied here, and SLP minima identified in the present analysis may include stationary features as well as cyclones (moving low-pressure systems). A test carried out by Hoskins and Hodges (2002) suggested that the planetary-scale background does not interfere significantly with variability of synoptic timescales, however, in some cases it may nevertheless be desirable to apply a filter to the data prior to the CCI. The CCI method can also be used to identify high-pressure systems (blocking) if criteria $\partial^2 p/\partial x^2 < 0$ and $\partial^2 p/\partial y^2 < 0$ are used, or to identify local maxima/minima in other data fields.

The analysis was done in the `R` environment (Ellner, 2001; Gentleman and Ihaka, 2000) which is freely available from the Comprehensive R Archive Network (CRAN) Internet site[1]. The CCI method and the database are freely available in the contributed `R`-package `cyclones` (open source code).

3. Results

3.1. Sensitivity studies and quality control

It is important to assess the robustness of the storm characteristics with respect to the different choices made in the CCI method. Figures 3(a)–(i) shows comparisons between different storm characteristics derived making different choices. The panels a–c show the scatter plots of longitudes, latitudes and storm centre pressures for the strongest cyclone at any given time obtained from the two different data sets (NMC ds195.5 and ERA40, both taken at 12 UTC). When many weaker subsidiary cyclones are included (not shown), the agreement is not as good. There are some differences in the storm characteristics, especially with respect to the storm centre pressure. A linear regression was used to quantify the similarities between the quantities plotted along the abscissa (x-axis) and ordinate (y-axis), using the standard R^2-statistics to indicate the similarity. The R^2-values of 88%, 74%, and 50% for longitudes, latitudes and pressure respectively, suggested a rough agreement on the location of the cyclones derived from the different data sources, and lesser agreement on the

[1]URL: http://cran.r-project.org.

central pressure of the individual storms. The ERA40 data yields more storms with extremely low central pressure (e.g. below 960 hPa) than the NMC data. The lowest storm centre pressure obtained from the ERA40 data was 920 *hPa* for 8 February 1959, which is an outlier. The location and intensity of this cyclone can be seen in Fig. 4a, showing it is a 'real feature' in the data set, but it was not seen in the NMC data with such an extreme value (there is a corresponding cyclone, but much shallower ~952–953 hPa), and Fig. 4b indicates that this event was unique. No reports could be found of such an extreme event, nor was this particular incident discussed in O'Connor (1959), so it cannot be ruled out that this exceptionally low value is a result of an error in the ERA40 data set. On the other hand, there is no obvious erroneous observations and the cyclone development is consistent with the physical conditions.

Similar sensitivity analysis as in panels (a)-(c) was applied to results obtained from the ERA40 SLP results, using different resolutions for interpolation rather than different data sources (panels d–f). This set of sensitivity tests involved using 0.5 and 1 degree step sizes for $\delta\theta$ and $\delta\phi$, which determine the spatial resolution of θ and ϕ in equation 1. The scatter plots in panels (d)-(f) indicate that the results are not very sensitive to the choice of resolution in the interpolation, as the R^2-values obtained for the longitudes, latitudes and storm centre pressure were 99%, 100% and 100% respectively.

Figure 3g shows how different choices of N_ϕ and N_θ affect the solutions for the central storm pressure. Here results using $N_\phi = N_\theta = 25$ were compared with $N_\phi = N_\theta = 10$, and the agreement is generally good. Similarly for longitudes and latitudes (not shown), the number of harmonics above 10 does not alter the results significantly.

Figure 3(h) shows a comparison between the maximum wind speed obtained through the four different methods described above and from the ERA40 data. The range of values are 0–35 m s^{-1} (0–125 km hr^{-1}) for the points of inflexion methods (ii and iv) and 0–80 m s^{-1} (0–290 km hr^{-1}) for the winds taken within a 5 degree radius (methods i and iii). The gradient wind formula yielded higher values than merely using the geostrophic wind equation. The range of wind speeds derived using methods (i) and (iii) is unrealistic, and the agreement between using the points of inflexion and 5 degree radius is poor for the maximum wind estimates ($R^2 \approx 1\%$). Hence, there is a significant difference between the two types of methodologies.

The relationship between the central storm pressure and the maximum wind was explored for both methods (i) and (iii) and methods (ii) and (iv) (Fig. 3i). The R^2-statistics suggest that methods (ii) and (iv) ($R^2 = 17$–18%) give a stronger relationship to the central pressure than do methods (i) and (iii) ($R^2 = 5$–6%). Since an association between the depth of the low pressure system and the maximum wind is presumed, and the range of wind speed obtained from methods (ii) and (iv) is more realistic, the point-of-inflexion method is considered superior (and is the approach used in the `cyclones` package).

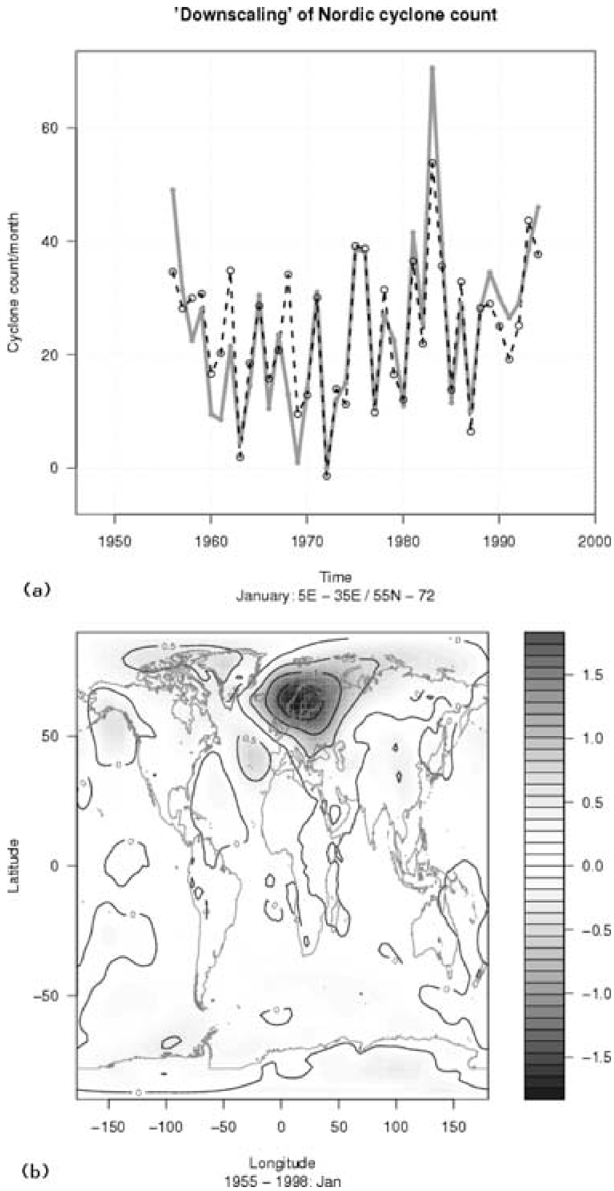

Fig. 6. Using January SLP to downscale the cyclone count (threshold set at 1000 hPa) over the Nordic countries. (b) Spatial structure shows a consistent picture between the cyclone counts obtained here and the monthly mean SLP NCEP re-analysis.

Figure 4c shows a case study for the famous Great Storm of 15–16 October 1987. The location of the storm centres in the CCI-results is in good agreement with historical accounts (Jarraud et al., 1989, fig. 4).

Figure 5 presents a map of cyclone density (mean count/month for the whole year) for the period 1955–1994 derived from both NMC (contours left) and NMC-ERA40 difference (right), and well-known regions of high storm-activity can be seen in both results. Similar maxima near Iceland and Newfoundland can be seen in the cyclone track density analysis by Sorteberg

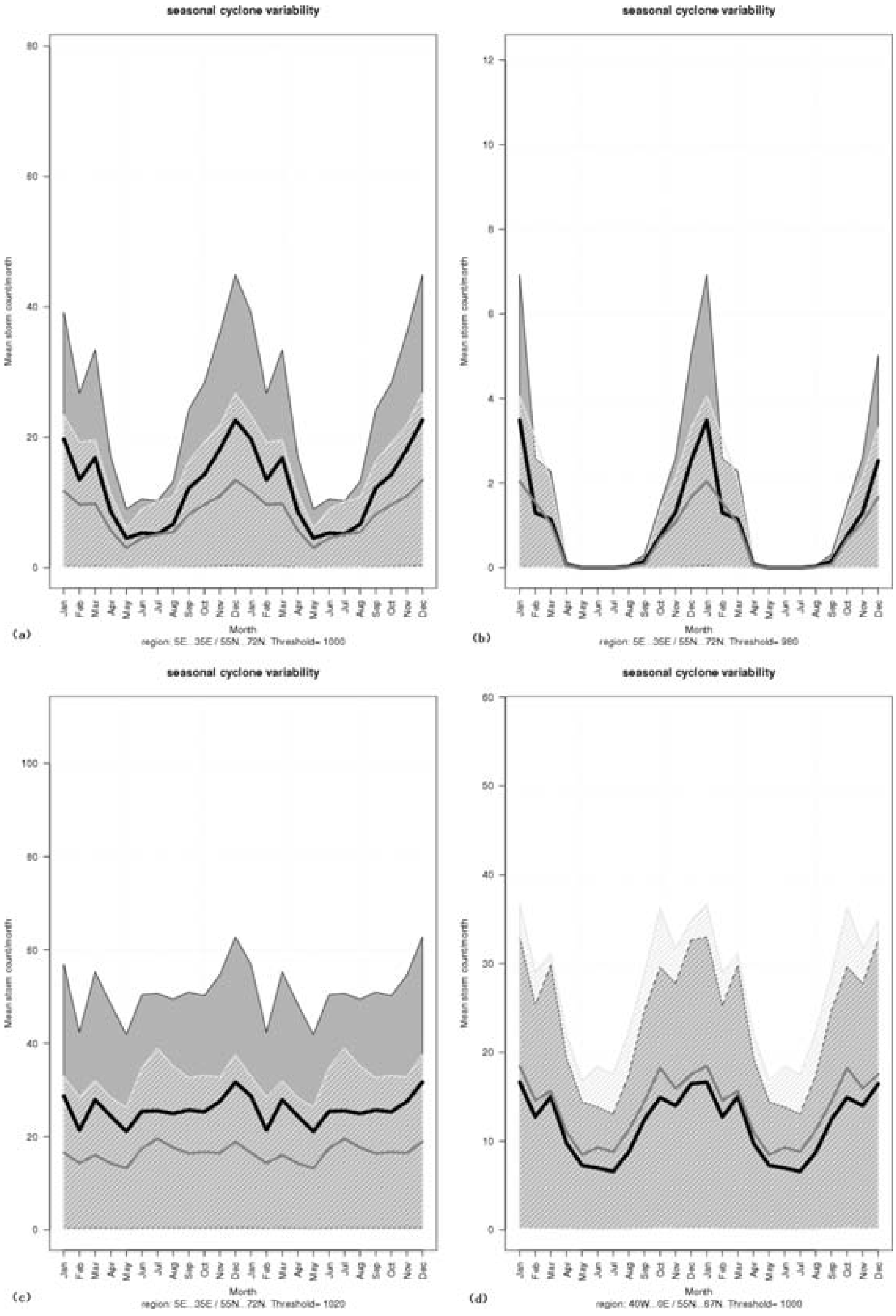

Fig. 7. Seasonal cyclone-count variations for (a) cyclone counts in the region 5° E–35° E, 55° N–72° N (inside box shown in Fig. 5) with local SLP minima < 1000 hPa, (b) cyclones with local SLP minima < 980 hPa for the same region, (c) cyclones with local SLP minima < 1020 hPa for the same region and (d) cyclones in 40° W–0° E,55° N–67° N with local SLP minima < 1000 hPa. The grey area marks ± 1 standard deviation. Thick dark curve shows NMC results whereas thick grey curve shows ERA40 (1 × 1). Solid grey region marks the mean ± standard deviation for the NMC results whereas the transparent hatched region marks the corresponding ERA40 spread.

et al. (2005) (their Figure 1), Hoskins and Hodges (2002) (their Figure 3), and the cyclone frequency obtained by Gulev et al. (2001) (their Figure 1). The general storm count from the NMC and ERA40 re-analysis were consistent in the storm track region south of Greenland and west of Iceland, but the NMC analysis yielded higher storm frequencies over Fennoscandia. The map in Fig. 5a also suggests a high number of cyclone counts over northern Finland, the Kola peninsula and the bordering Barents Sea, and both results from NMC and ERA40 contain a particularly high count over the Norwegian Barents Sea border.

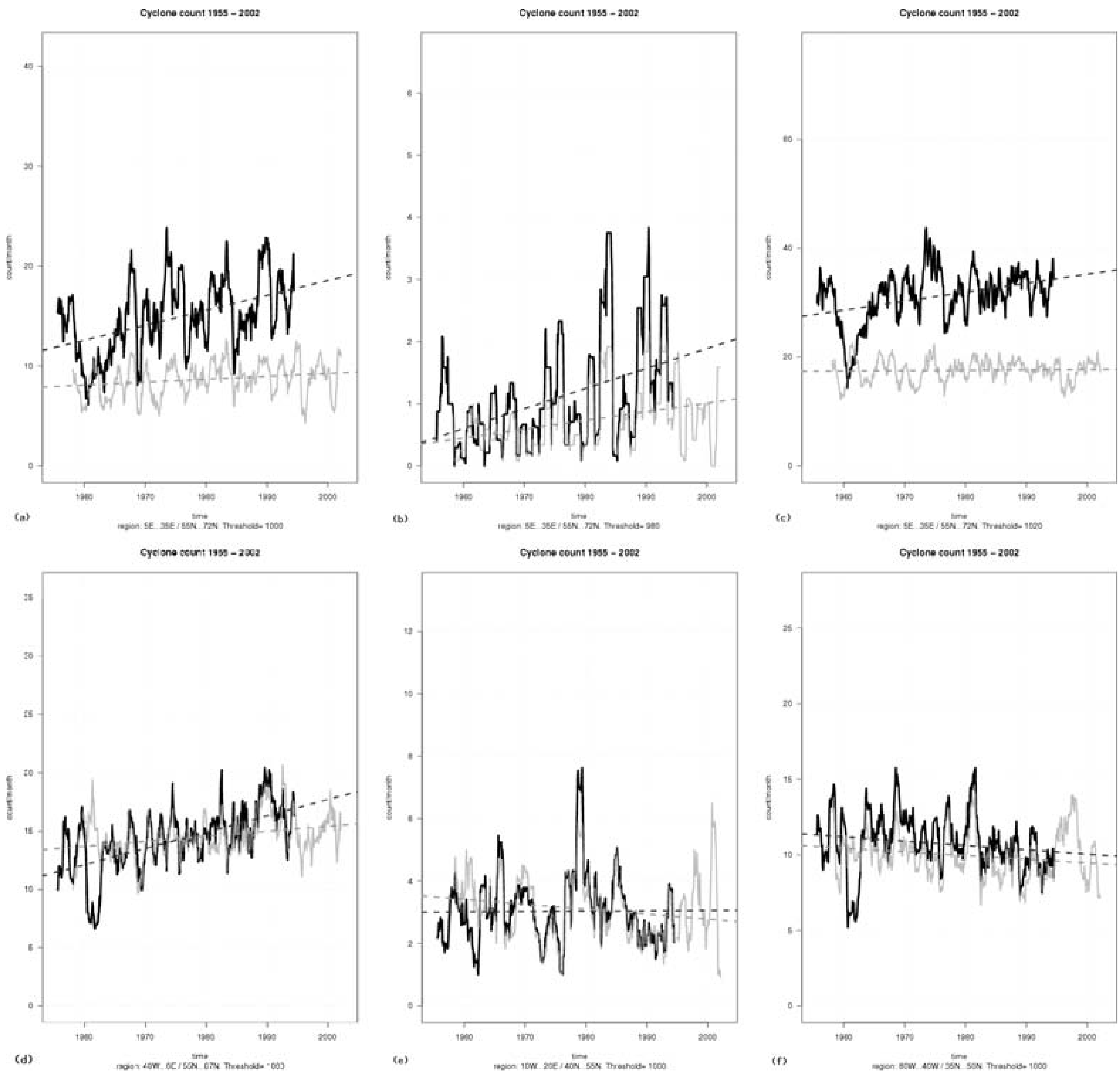

Fig. 8. Time-series of the cyclone semi-day count for (a) in the 5° E–35° E/55° N–72° N (Nordic) region with local SLP minima < 1000 hPa, (b) cyclones with local SLP minima < 980 hPa for the same region, (c) cyclones with local SLP minima < 1020 hPa for the same region, (d) cyclones in 40° W–0° E,55° N–67° N (Iceland) with local SLP minima < 1000 hPa, (e) 10° W–20° E, 40° N–55° N (continental Europe) with local SLP minima < 1000 hPa, (f) 80° W–40° W, 35° N–50° N). The monthly storm counts have been smoothed by taking the 12 month running average.

Zhang et al. (2004) found a high cyclone count in the same vicinity during winter, but they found also similar ‘hotspots’ south of Svalbard, and southeast of Greenland (their Fig. 2a). The analysis by Gulev et al. (2001) suggests substantial cyclone activity over the Barents Sea whereas the cyclone density by Sorteberg et al. (2005) indicates a local maximum over the Baltics, but none of these match the high counts suggested by the present analysis. One explanation for this high number may be that the cyclones move more slowly in this region or veer off as the storms hit land, enhancing the monthly count. Another difference may be that the present analysis does not distinguish between stationary features and moving cyclones for high-latitude regions where the meridional lines converge. It is clear from a comparison with a similar map for deeper cyclones (Fig. 5b) that the high count over the Barents Sea region is mostly due to weaker cyclones.

The cyclone counts can be further evaluated through a compilation of a time-series for the number of low pressure systems falling within the region 5° E–35° E, 55° N–72° N (inside box shown in Fig. 5, henceforth denoted as the ‘Nordic region’), and using this time-series as the predictand in a downscaling analysis together with predictors consisting of monthly NCEP SLP fields. Here we use a rectangular longitude-latitude region, although Sepp et al. (2004) and references therein recommend using a circular region for more accurate estimates. Figure 6 shows results from such an analysis performed for the January month. The high variance ($R^2 = 78\%$) obtained for the regression of the global-scale SLP onto the time-series of the cyclone counts in the Nordic region (based on the NMC data) indicates a strong statistical relationship between these two variables. The ERA40 results gave a similar figure (not shown). The analysis also shows that the reconstructed (downscaled, black dashed) time-series follows the 'observed' (grey) counts closely (Fig. 6a). The weightings of the SLP in Fig. 6b point to negative values over the Nordic region consistent with a high count of low pressure systems in the same area.

The seasonal dependency of the cyclone count is shown in Fig. 7 for different thresholds and regions. The more intense cyclones (b) over the Nordic countries are more frequent in winter, in accordance with expectations, and weak (panel c) low-pressure systems do not have a well-defined seasonality. Figure 7d shows the seasonal dependency of cyclone counts over Iceland (40° W–0° E,55° N–67° N), which indicates a longer lasting ('flatter') stormy season than over 5° E–35° E, 55° N–72° N. The seasonal variation is slightly more pronounced in the NMC results (thick black) than in the ERA40 estimates (thin dark grey). The NMC results indicates a higher cyclone activity over the Nordic region than ERA40, but over Iceland (Fig. 7d) the NMC and ERA40 yield similar cyclone counts. The seasonal variations in Figs 7(a)–(d) contrast with the Arctic storm statistics, as Zhang et al. (2004) found the cyclone trajectory count in the Arctic to be higher in summer as well as the cyclone duration being longer during summer. However, this analysis precludes the Arctic, and here cyclone counts are assessed rather than cyclone trajectory counts.

Table 1 presents cross-correlations between cyclone counts from different regions and for different threshold values. There is a significant (at the 5% level) correlation between the storm activity around Iceland and over the Nordic countries, but not between the Nordic countries and the continental Europe. It is also interesting to note a correlation of 0.36 between Newfoundland (70° W–30° W,50° N–65° N) and the Nordic countries, correlations of 0.25 and 0.42 for intense and weak Nordic cyclones respectively, and a negative correlation (−0.39) between 'subtropical storms' (80° W–30° W, 35° N–50° N, threshold =970 hPa) and deep Nordic cyclones.

3.2. *Historic long-term trend*

Several studies have revealed results that caution against using re-analyses in studying trends (Hines et al., 2000; Harnik and Chang, 2003; Bengtsson et al., 2004; Smits and Können, 2005), as Harnik and Chang (2003) suggested that the NCEP-NCAR re-analysis indicate a stronger intensification of the north Atlantic storm track than radiosondes, Bengtsson et al. (2004) observed that changes in the number of global observations affect the estimates of atmospheric humidity and kinetic energy, and Smits and Können (2005) found different trends in storminess in either the NCEP and the ERA40 re-analysis when comparing with wind data from Dutch meteorological stations. It is nevertheless useful to carry out trend analysis using re-analyses, but it is important to keep these caveats in mind. Furthermore, applying a filter to isolate the high-frequency synoptic variability from the slowly changing background field may also affect the trend analysis.

The cyclone statistics derived from the (raw) NMC data (black) over the Nordic countries, region 5° E–35° E/55° N–72° N, indicate a positive linear trend with time in cyclones deeper than 1000 hPa (Fig. 8a), suggesting an increase of 1.6 cyclones/decade for the entire year with an estimated *p*-value= 0.00236 (grey region in Fig. 5). However, a corresponding trend for January is not statistically significant according to Fig. 8a, and the ERA40 data (grey) do not suggest a systematic long-term trend. A long-term trend can also be seen in the number of intense (central pressure below 980 hPa) cyclones over the Nordic region (b), in this case in both NMC and ERA40. Only the NMC results suggest long-term trends over weak Nordic cyclones (very weak) and over Iceland (Figs 8c and d). Similar analysis for the continental Europe (10° W–20° E, 40° N–55° N) and the western part of the North Atlantic (80° W–40° W, 35° N–50° N, near Bermuda), on the other hand, suggest an insignificant long-term trend in the NMC and a long-term decline in the ERA40 results (Figs 8e and f). Table 2 gives a summary of cyclone count trends in different regions and for different threshold pressure, and it is important to take all the estimates into account when estimating the field significance of the long-term change in the storm behaviour for the entire Atlantic basin. It is also important to keep in mind that field significance tests may fail to capture real local changes such as a shift in the storm track position. The trends here were computed for monthly values, so that seasonal variations make a contribution to the total variance and makes the significance estimates more conservative than if the annual cycle was removed (i.e. the *p*-value is 0.002 for the annual storm count in the Nordic region). The table reveals important differences between the two data sets, and the cyclone count for the entire North Atlantic (80° W–40° E/20° N–50° N) favours the notion of an increase in the intense storm frequency only in the NMC data. The trends found here nevertheless were in general agreement with the results of Sepp et al. (2004), who used the method of Gulev et al. (2001) applied to the 6 hr NCEP/NCAR re-analysis data over the Nordic countries.

4. Discussion and Conclusions

A new method for identifying cyclones, CCI, was proposed, and an evaluation of results derived using this approach suggests that it skilfully identifies the past storm characteristics. The CCI also returns estimates for maximum wind speed, storm radius, and SLP gradients. Thus, the advantages of the CCI method over more traditional ones are: (i) yields estimates of gradients, gradient winds, and geostrophic winds; (ii) provides a higher precision of cyclone location; (iii) returns an objective estimate of physical size and (iv) is less sensitive to small-scale noise. It is shown that the annual variation and the long-term trends in regional storminess can be sensitive to the choice of data set, and hence, the present findings are consistent with different temporal evolution of cyclones reported by Hanson et al. (2004). There may be time-varying biases in the re-analysis products, and re-analysis trends should therefore not be taken at face value without independent verification (Hines et al., 2000). Here, spatially interpolated monthly mean SLP from ERA40 was compared with corresponding measurement from the Nordklim data set (Tuomenvirta et al., 2001) for Jan Mayen, Oslo, Stykkisholmur, Svalbard airport, Tromsø, Vardø, Ship 'M', Hammerodde lighthouse, Sodankylä, Helsinki, and Torshavn respectively (not shown), demonstrating a close agreement between the re-analysis and station observations. No discrepancies in trend were seen. It is not possible to apply a similar test for the vorticity, as we have no similar empirical measurements. It is important to stress that caution should be taken when interpreting the cyclone trends found in re-analysis products, as Smits and Können (2005) found a 10% decrease in storminess over the Netherlands over the 1962–2002 period in the Dutch meteorological stations that were inconsistent with the increase in long-term storminess derived from NCEP-NCAR and ECMWF re-analyses (in terms of wind products). It should also be noted that they derived storminess statistics in the re-analyses from geostrophic winds using a so-called triangle method applied to adjacent grid boxes and that present results suggest geostrophic winds do not have a good correspondence with the storms' central pressure. The negative trends found here, albeit for a larger region, are more consistent with their trends based on the meteorological stations than their results based on the re-analyses. We found one exceptionally deep cyclone in the ERA40 data, which could be an indication that the ERA40 contains serious errors in terms of storm centre pressure, but this question has yet not been resolved. The wind estimates were also found to be sensitive to the choice of method, whereas the location and depth of the storms are not very sensitive to CCI set-up.

5. Acknowledgment

This work was done under the Norwegian Regional Climate Development under Global Warming (RegClim) programme, and was supported by the Norwegian Research Council (Contract NRC-No. 120656/720), the Norwegian Meteorological Institute, China Meteorological Administration (CCSF2006-6), and the Swedish Science Council and the Swedish Rescue Services Agency. The analysis was carried out using the R (Ellner, 2001; Gentleman and Ihaka, 2000) data processing and analysis language, which is freely available over the Internet (URL http://www.R-project.org/). We are also grateful for valuable discussions and comments from Asgeir Sorteberg, Ivar Seierstad, John Walsh and Amanda Lynch and valuable comments from two anonymous reviewers.

References

Agee, E. M. 1991. Trends in cyclone and anticyclone frequency and comparison with periods of warming and cooling over the Northern Hemisphere. *J. Climate* **4**, 263.

Alexander, M., Bhatt, U., Walsh, J., Timlin, M., Miller, J. and co-authors. 2004. The Atmospheric Response to Realistic Actic Sea Ice Anomalies in an AGCM during winter. *J. Climate* **17**, 890.

Alpert, P., Neeman, U. and Shau-El, Y. 1990. Interannual variability of cyclone tracks in the Mediterranean. *J. Climate* **3**, 1474.

Benestad, R. 1998. Klima 24/98, Description and Evaluation of the Predictor Data sets used for Statistical Downscaling in the RegClim. DNMI, PO Box 43 Blindern, 0313 Oslo, Norway.

Benestad, R. 2003. What can present climate models tell us about climate change?. *Climati. Change* **59**, 311.

Benestad, R. 2004. Empirical-Statistical Downscaling in Climate Modeling. *Eos*, Volume **85**, p. 417.

Benestad, R. and Hanssen-Bauer, I. 2003. KLIMA 07/03, Empirical-based refinement of dynamically downscaled temperature scenarios in southern Norway. The Norwegian Meteorological Institute, PO Box 43 Blindern, 0313 Oslo, Norway (www.met.no).

Bengtsson, L., Hagemann, S. and Hodges, K. 2004. Can climate trends be calculated from reanalysis data?. *J. Geophys. Res.* **109**.

Blender, R., Fraedrich, K. and Lunkeit, F. 1997. Identification of cyclone track regimes in the North Atlantic. *Qtr. J. Royal Met. Soc.* **123**, 727.

Blender, R. and Schubert, M. 2000. Cyclone tracking in different spatial and temporal resolutions *Monthly Weather Review* **128**, 377.

Carnell, R. and Senior, C. 1998. Changes in mid-latitude variability due to increasing greenhouse gases and sulphate aerosols *Climate Dynamics* **14**, 369.

Ellner, S. 2001. Bulletin of the Ecological Society of America. **82**, 127.

Fleagle, R. and Businger, J. 1980. *An Introduction to Atmospheric Physics*, 2nd Edition. Vol. 25 of International Geophysics Series, Academic Press, Orlando.

Fyfe, J. 2003. Extratropical Southern Hemisphere Cyclones: Harbingers of Climate Change?. *J. Climate* **16**, 2802.

Geng, Q. and Sugi, M. 2001. Variability of the North Atlantic Cyclone Activity in Winter Analyzed from NCEP-NCAR Reanalysis data. *J. Climate* **14**, 3863.

Geng, Q. and Sugi, M. 2003. Possible Change of Extratropical Cyclone Activity due to Enhanced Greenhouse Gases and Sulfate Aerosols – Study with a High-Resolution AGCM. *J. Climate* **16**, 2262.

Gentleman, R. and Ihaka, R. 2000. Lexical Scope and Statistical Computing *Journal of Computational and Graphical Statistics* **9**, 491.

Gill, A. 1982.. *Atmosphere-Ocean Dynamics*. Academic Press, San Diego, California, USA.

Graham, N. and Diaz, H. 2001. Evidence for intensification of North Pacific Winter Cyclones since 1948 *Bull. Amer. Meteor. Soc.* **82**, 1869.

Grigoriev, S., Gulev, S. and Zolina, O. 2000. Innovative software facilitates cyclone tracking and analysis *Eos* **81**, 170.

Gulev, S., Zolina, O. and Grigoriev, S. 2001. Extratropical cyclone variability in the Northern Hemisphere winter from the NCEP/NCAR reanalysis data *Climate Dynamics* **17**, 795.

Hall, N., Hoskins, B., Valdes, P. and Senior, C. 1994. Storm tracks in a high resolution GCM with doubled CO_2 *Qtr. J. Royal Met. Soci.* **120**, 1209.

Hanson, C., Palutikof, J. and Davies, T. 2004. Objective cyclone climatologies of the North Atlantic - a comparison between the ECMWF and NCEP Reanalyses *Climate Dynamics* **22**, 757.

Harnik, N. and Chang, E. 2003. Storm Track Variations As Seen in Radiosonbde Observations and Reanalysis Data. *J. Climate* **16**, 480.

Hines, K., Bromwich, D. and Marshall, G. 2000. Artificial Surface Pressure Trends in the NCEP-NCAR Reanalysis over the Southern Ocean and Antarctica. *J. Climate* **13**, 3940.

Hodges, K. 1994. A General Method for Tracking Analysis and Its Application to Meteorological Data *Monthly Weather Review* **122**, 2573.

Hodges, K. 1995. Feature Tracking on the unit sphere. *Monthly Weather Review* **123**, 3458.

Hodges, K. 1999. Adaptive Constraints for Feature Tracking *Monthly Weather Review* **127**, 1362.

Hoskins, B. and Hodges, K. 2002. New Perspectives on the Northern Hemisphere Winter Storm Tracks *J. Atmospher. Sci.* **59**, 1041–1061.

Hoskins, B. and Hodges, K. 2005. A New Prespective on Southern Hemisphere Storm Tracks. *J. Climate* **18**, 4108.

Jarraud, M., Cyoas, J. and Deyts, C. 1989. Prediction of an Exceptional Storm over France and Southern England (15 \ u201316 October 1987. *Weather and Forecasting* **4**, 517.

Jones, D. A. and Simmonds, I. 1993. A climatology of Southern Hemisphere extratropical cyclones *Climate Dynamics* **9**, 131.

Jung, T., Gulev, S., Rudeva, I. and Soloviov, V. 2006. Research Dept., Technical Memorandum 485, Sensitivity of extratropical cyclone characteristics to horizontal resolution in the ECMWF model. ECMWF.

Kalnay, E., Kanamitsu, M., Kistler, R., Collins, W., Deaven, D. and co-authors1996. The NCEP/NCAR 40-Year Reanalysis Project. *Bull. Amer. Meteor. Soc.* **77**, 437.

Key, J. and Chan, A. 1999. Multidecadal global and regional trends in 1000 mb and 500 mb cyclone frequencies *Journal of Geophysical Research* **26**, 2053.

Leonard, S., Turner, J. and der Wal, A. V. 1999. An assessment of three automatic depression tracking schemes *Meteorological Applications*, **6**, 173.

Meier, W., Stroeve, J., Fetterer, F. and Knowles, K. 2005. Reductions in Arctic Sea Ice Cover No Longer Limited to Summer *Eos* **86**, 326.

Mohn, H. 1870. Det Norske Meteorologiske Instituts Storm-Atlas *Centen. Proc. Roy. Met. Soc.* **17**, 26.

Murray, R. and Simmonds, I. 1991. A numerical scheme for tracking cyclone centres from digital data. Part I: development and operation of the scheme. *Aust. Met. Mag.* **39**, 155.

O'Connor, J. 1959. Technical report, The weather and circulation of February 1959. Extended Forecast Section, U.S. Weather Bureau, Washington, D.C.

Peixoto, J. and Oort, A. 1992. *Physics of Climate*. AIP, N.Y.

Petterssen, S. 1950. Some aspects of the general circulation. *Centen. Proc. Roy. Met. Soc.* **17**, 120.

Rew, R., Davis, G., Emmerson, S. and Davies, H. 1996. NetCDF User's Guide. Unidata Program Center, http://www.unidata.ucar.edu/packages/netcdf/.

Schubert, S. 1998. Downscaling local extreme temperature change in south-eastern Australia from the CSIRO MARK2 GCM *Int. J. Climatol.* **18**, 1419.

Sepp, M., Post, P. and Jaagus, J. 2004. Long-term changes in the frequency of cyclones and their trajectories in Central and Northern Europe *Nordic Hydrology* **36**, 297.

Simmonds, I. and Keay, K. 2000. Variability of Southern Hemisphere extratropical cyclone behavior, 1958-97. *J. Climate* **13**, 550.

Simmonds, I. and Murray, R. 1999. Southern Extratroical Cyclones Behaviour in ECMWF Analyses during the FROST Special Observing Periods *Weather and Forecasting* **14**, 878.

Simmons, A., Jones, P., da Costa Bechtold, V., Beljaars, A., Kållberg, P. and co-authors. 2004. ERA40 Project Report Series 18, Comparison of trend and variability in CRU, ERA40 and NCEP/NCAR analyses of monthly-mean surfaceair temperatures. ECMWF.

Simmons, A. J. and Gibson, J. K. 2000. Era-40 project report series, The ERA-40 Project Plan. ECMWF.

Smits, A. A. K. T. and Können, G. 2005. Trends in storminess over the Netherlands, 1962–2002. *International Journal of Climatology*, **25**, 1331.

Sorteberg, A., Kvamstø N. and Byrkjedal Ø. 2005. Wintertime Nordic Seas Cyclone Variability and its Impact on Oceanic Volume Transport Into the Nordic Seas; The Nordic Seas: An integrated Perspective.

Trenberth, K. 1991. Some aspects of the general circulation *Journal of the Atmospheric Sciences* **48**, 2159.

Tuomenvirta, H., Drebs, A., Førland, E., Tveito, O., Alexandersson, H. and co-authors. 2001. KLIMA 08/01, Nordklim data set 1.0. met.no, P.O. Box 43 Blindern, N-0313 Oslo, Norway (www.met.no).

Ulbrich, U. and Christoph, M. 1999. A shift in the NAO and increased storm track activity over Europe due to anthropogenic greenhouse gas forcing *Climate Dynamics*, pp. 551–559.

Uppala, S., Kallberg, P., Simmons, A., Andrae, U., da Costa Bechtold, V. and co-authors. 2005. The ERA-40 re-analysis *Quart. J. Roy. Meteor. Soc.* **131**, 2961.

Walsh, K. 2004. Tropical cyclones and climate change: unresolved issues *Climate Research* **27**, 77.

Zhang, X., Walsh, J., Zhang, J., Bhatt, U. and Ikeda, M. 2004. Climatology and Interannual Variability of Arctic Cyclone Activity: 1948-2002 *J. Climate* **17**, 2300.

Zolina, O. and Gulev, S. 2002. Improving the Accuracy of Mapping Cyclone Numbers and Frequencies *Mon. Weather Rev.* **130**, 748.